Journal of Mechanics Engineering and Automation 2 (2012) 709-719

# Angle Control of a Pneumatically Driven Musculoskeletal Model Based on Coordination of Agonist-Antagonist Muscle

Yuki Honda[1], Fumio Miyazaki[1] and Atsushi Nishikawa[2]

*1. Department of Mechanical Science and Bioengineering, Graduate School of Engineering Science, Osaka University, Toyonaka 560-8531, Japan*

*2. Bioengineering Course, Division of Mechanical Engineering and Robotics, Faculty of Textile Science and Technology, Shinshu University, Ueda 386-8567, Japan*

Received: November 19, 2012 / Accepted: December 15, 2012 / Published: December 25, 2012.

**Abstract:** In recent years, researchers have been actively pursuing research into developing robots that can be useful in many fields of industry (e.g., service, medical, and aging care). Such robots must be safe and flexible so that they can coexist with people. Pneumatic actuators are useful for achieving this goal because they are lightweight units with natural compliance. Our research focuses on joint angle control for a pneumatically driven musculoskeletal model. In such a model, we use a one-degree-of-freedom joint model and a five-fingered robot hand as test beds. These models are driven by low pressure-driven pneumatic actuators, and mimic the mechanism of the human hand and musculoskeletal structure, which has an antagonistic muscle pair for each joint. We demonstrated a biologically inspired control method using the parameters antagonistic muscle ratio and antagonistic muscle activity. The concept of the method is based on coordination of an antagonistic muscle pair using these parameters. We have investigated the validity of the proposed method both theoretically and experimentally, developed a feedback control system, and conducted joint angle control by implementing the test beds.

**Key words:** Musculoskeletal model, pneumatic actuator, position control, muscle coordination, agonist-antagonist muscle.

## 1. Introduction

Research into developing robots that can coexist with people in service, medical, and aging care industries has been active in recent years. Such robots must be safe because they work directly with humans [1]. Pneumatic actuators have gained much attention for achieving this goal because they are lightweight units with natural compliance [2]. Our research focuses on human-like robotic joints fitted with pneumatic actuators to mimic the mechanism of the human musculoskeletal structure.

The human musculoskeletal structure consists mainly of bones, and agonist and antagonist muscles. These muscles work in a pair called an antagonistic muscle pair. The joint movement is coordinated by the pair of muscles: one muscle, called the flexor, contracts to bend the joint, while the other, called the extensor, stretches. The extensor, in turn, contracts to stretch the flexor, resulting in straightening the joint.

According to Bernstein, humans use muscle synergy, which coordinates a group of muscle to control the human redundant structure [3]. Also, the human antagonistic muscle pairs contract simultaneously, although the use of one muscle is

Yuki Honda, graduated student (presently employed at Yaskawa Electric Corporation, Japan), research field: robotics.

Fumio Miyazaki, professor, Ph.D., research fields: robotics, human-robot interaction.

**Corresponding author:** Atsushi Nishikawa, professor, Ph.D., research fields: biomechatronics and medical robotics. E-mail: nishikawa@shinshu-u.ac.jp.

sufficient while bending a joint [4].

The objective of our research is to develop a control method inspired by such an anatomical mechanism, and to incorporate this method into a robotic musculoskeletal model. The basis of the control method is the coordination of the antagonistic muscle pair. Our proposed biologically inspired control method uses the parameters antagonistic muscle ratio and antagonistic muscle activity. The antagonistic muscle ratio is defined as the ratio of air pressures between the extensor and the sum of the extensor and the flexor. Antagonistic muscle activity is defined as the sum of air pressures of the extensor and the flexor. Since the coordination of an antagonistic muscle pair of the pneumatic actuators is based on these parameters, it is necessary to explore the relationship between joint angle and coordination.

Previous studies suggest joint angle control methods for a robotic joint driven by antagonistic pairs of pneumatic actuators. Tsujiuchi et al. developed a proportional-integral-derivative (PID) control system with highly accurate performance [5]. However, it activates only one actuator while bending a joint, resulting in invariable joint stiffness. Many researchers employ the classical angle control approach, which uses the difference in pressure between the agonist and antagonist as a control command [6-7]. For example, Tondu et al. derived the relationship between joint angle and difference in pressure [2]. However, parameters of actuators are necessary to derive this relationship, since the relationship between angle and difference in pressure depends on the actuator properties. To describe the relationship between joint angle and control command more universally, our research explores the relationship between joint angle and muscle coordination. We implement joint angle control by using two types of pneumatically driven musculoskeletal models: a one-degree-of-freedom joint model and a five-fingered robot hand.

In this study, we propose a control method using the new parameters, after introducing pneumatic actuators and musculoskeletal models. We then implement the method in a one-degree-of-freedom joint model, in order to validate the proposed method. Furthermore, we expand the method into a proportional-integral-derivative (PID) feedback control system and conduct joint angle control using the model, and then implement the feedforward method in the index finger of the five-fingered robot hand.

## 2. Pneumatically-Driven Musculoskeletal Model

### *2.1 Low Pressure-Driven McKibben Pneumatic Actuator*

A McKibben pneumatic actuator is an artificial muscle that generates axial tension from air pressure. It consists of a rubber inner tube and a braided shell. The actuators developed by SQUSE Co., Ltd., are more compact, light-weight, and low pressure-driven than other conventional models because their rubber inner tubes are thinner and softer [8]. Using a relatively small compressor, the actuators can be fitted directly in the pneumatically driven robots, enabling size reduction of the driving system. Fig. 1 depicts the McKibben pneumatic actuators embedded in a finger of the five-fingered robot hand. Table 1 presents a brief specification of the McKibben pneumatic actuators. For more technical details, see Ref. [8].

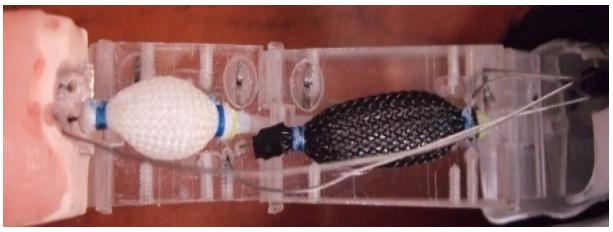

**Fig. 1 McKibben pneumatic actuator.**

**Table 1 Specifications of McKibben pneumatic actuator.**

| Category | Quantity |
|---|---|
| Maximum length | 18 to 90 mm |
| External diameter of air tube | 2 mm |
| Weight | 1 g (approximate) |
| Rated pressure | 0.2 MPa |

### *2.2 One-Degree-of-Freedom Joint Model*

To verify the proposed control method, we developed a one-degree-of-freedom joint model. In an ideal joint model, the joint moves symmetrically, and the two embedded actuators have the same properties.

Fig. 2 depicts the one-degree-of-freedom joint model. Table 2 presents the model specifications, and Table 3 indicates the properties of the McKibben pneumatic actuator embedded in the model.

### *2.3 Five-Fingered Robot Hand*

To apply the musculoskeletal model, we used SQUSE robot hand type-G developed by SQUSE Co., Ltd. This five-fingered robot hand is built to mimic a human hand. It contains an antagonistic muscle pair for each joint that is driven by the pneumatic actuators.

The actuators were placed to move the following joints: DIP, PIP, and MP joints of the index, the middle, and the ring fingers; PIP and MP joints of the little finger; and IP, MP, CMC joints of the thumb. The two pairs of actuators on the CMC joint of the thumb enable flexion, extension, and inner and outer rotations.

Fig. 3 illustrates the manipulator parts of the five-fingered robot hand. Table 4 indicates the specifications of the five-fingered robot hand.

## 3. Control Method Using Antagonistic Muscle Ratio and Antagonistic Muscle Activity

### *3.1 Ideal Joint Model*

In an ideal joint model, we assume that the properties of the extensor and the flexor are the same. The joint model has a one-degree-of-freedom joint that has an antagonistic muscle pair made of McKibben pneumatic actuators. These actuators are connected with a driving pulley.

### *3.2 Definition of Antagonistic Muscle Ratio and Antagonistic Muscle Activity*

We define antagonistic muscle ratio (*Ar*) as the ratio of air pressures between the extensor and the sum of the extensor and the flexor. We define antagonistic

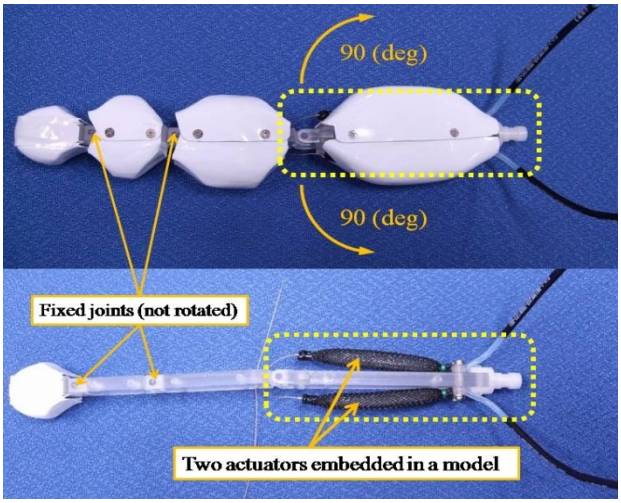


**Fig. 2 One-degree-of-freedom joint model. (upper: the model with exterior, lower: the plain model (no exterior)).**

**Table 2 Specifications of one-degree-of-freedom joint model.**

| Category | Quantity |
|---|---|
| Number of joints | 1 |
| Number of actuators | 2 |
| Maximum length of actuator | 45 mm (approximate) |
| Joint range of motion | 180deg |

**Table 3 Properties of McKibben pneumatic actuator (one-degree-of-freedom joint model).**

| Property | Extensor | Flexor |
|---|---|---|
| Maximum length | 44.6 mm | 45.0 mm |
| Contraction ratio | 31.6% | 32.4% |
| External diameter (during contraction) | 12.1 mm | 12.3 mm |
| Maximum contraction force | 28.5 N | 29.4 N |

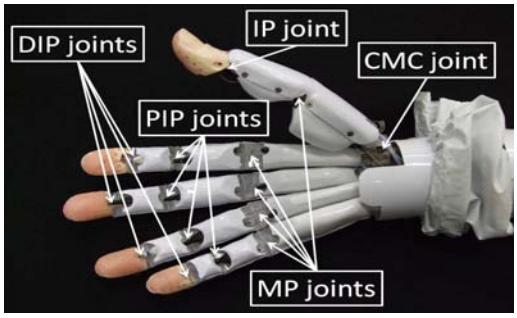


**Fig. 3 Five-fingered robot hand.**

**Table 4 Specifications of five-fingered robot hand.**

| Category | Quality or quantity |
|---|---|
| Material (bony framework) | Polycarbonate |
| Material (fingertip) | Silicon rubber |
| Weight | 400 g (approximate) |
| Number of actuators | 21 fingers, 4 wrists |
| Degrees of freedom | 17 |

muscle activity (*Ac*) as the sum of the air pressures of the extensor and the flexor [9-10]. *Ar* represents joint angle, while *Ac* represents joint stiffness. These parameters are given by

$$Ar \equiv \frac{P_e}{P_e + P_f} \tag{1}$$

$$Ac \equiv P_e + P_f = P \geq \overline{P} \tag{2}$$

where $P_e$ indicates air pressure of the extensor, $P_f$ indicates that of the flexor, and $\overline{P}$ denotes the minimum air pressure that enables the joint model to move its joint to the maximum and minimum angles.

Solving Eqs. (1) and (2) as simultaneous equations, $P_e$ and $P_f$ are expressed by

$$P_e = ArAc \tag{3}$$

$$P_f = (1 - Ar)Ac \tag{4}$$

### *3.3 Correspondence between Antagonistic Muscle Ratio and Joint Angle*

We examine the correspondence between *Ar* and joint angle. To design this correspondence, we introduce a joint model that has a maximum joint angle ($\theta_{max}$) of 90deg and a minimum joint angle ($\theta_{min}$) of -90deg. In Fig. 4, the first graph represents the state of the joint model for $Ar = 0$. In this state, we obtain $P_e = 0$, $P_f = Ac$ from Eqs. (3) and (4); thus, the joint angle is -90deg, since the joint model is considered to be fully flexed. The middle graph represents the state of the joint model for $Ar = 0.5$. In this state, we obtain $P_e = 0.5Ac$, $P_f = 0.5Ac$; thus, the joint angle is 0deg, since tension between the extensor and the flexor is considered to be the same. The last graph represents the state of the joint model for $Ar = 1$. In this state, we obtain $P_e = Ac$, $P_f = 0$; thus, the joint angle is 90deg, since the joint model is considered to be fully extended.

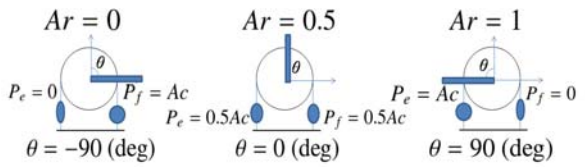


**Fig. 4 Example of correspondence between antagonistic muscle ratio and joint angle.**

From these examples, we obtain the correspondence between *Ar* and joint angle $\theta$ in three states: $\theta$ = -90 = $\theta_{min}$ when $Ar = 0$, $\theta = 0 = (\theta_{max} + \theta_{min})/2$ when $Ar = 0.5$, and $\theta = 90 = \theta_{max}$ when $Ar = 1$. If we assume that there is a linear relation between *Ar* and $\theta$, we obtain

$$Ar = \frac{\theta - \theta_{\min}}{\theta_{\max} - \theta_{\min}} \tag{5}$$

Using Eq. (5), we can derive air pressure from the desired joint angle $\theta$.

Since *Ar* represents joint angle and *Ac* represents joint stiffness, they are assumed to be independent. For example, the joint model can vary the joint stiffness while maintaining the joint angle.

### *3.4 Feedback Control Method*

In this section, we expand the proposed method into the PID feedback control. First, the control signal *u* is calculated by

$$u = K_P e + K_I \int_0^t e\,dt + K_D \frac{de}{dt} \tag{6}$$

Here, *e* is defined as the deviation between the desired joint angle and the measured joint angle.

*Ar* is then calculated by

$$Ar = \frac{u - \theta_{\min}}{\theta_{\max} - \theta_{\min}} \tag{7}$$

From Eq. (7) and a given *Ac*, the air pressure of the extensor and the flexor are determined by Eqs. (3) and (4). Fig. 5 presents a block diagram of the control method.

### *3.5 Implementation in Five-Fingered Robot Hand*

In this section, we explain how to implement the proposed method in the five-fingered robot hand.

The link model of the index finger of the robot hand is depicted in Fig. 6. Each joint has one degree of freedom, resulting in three degrees of freedom in each finger. However, each finger has only one extensor.

Now we solve the problem regarding air pressures $P_1$, $P_2$, $P_{3f}$, and $P_e$ for the desired angles of the DIP, PIP, MP joints, and the antagonistic muscle activity of the MP joint. The desired angles are represented by $\theta_1$ for the DIP joint, $\theta_2$ for the PIP joint, $\theta_3$ for the MP joint,

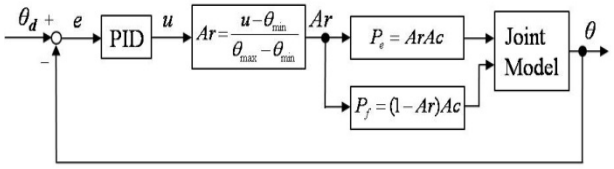


**Fig. 5 Feedback control system.**

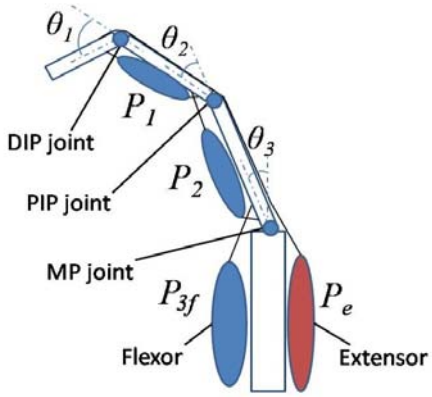


**Fig. 6 Link model of the index finger.**

and $Ac_3$ for the antagonistic muscle activity of the MP joint. Here, $Ac_3 = P_{3f} + P_e$.

First, we calculate the values of the antagonistic muscle ratios of DIP $(Ar_1)$, PIP $(Ar_2)$, and MP joints $(Ar_3)$. From Eq. (5), we get

$$Ar_1 = \frac{\theta_1 - \theta_{1\min}}{\theta_{1\max} - \theta_{1\min}} \tag{8}$$

$$Ar_2 = \frac{\theta_2 - \theta_{2\min}}{\theta_{2\max} - \theta_{2\min}} \tag{9}$$

$$Ar_3 = \frac{\theta_3 - \theta_{3\min}}{\theta_{3\max} - \theta_{3\min}} \tag{10}$$

From Eqs. (3) and (4), we get

$$P_e = Ar_3 Ac_3 \tag{11}$$

$$P_{3f} = (1 - Ar_3) Ac_3 \tag{12}$$

Since this model has only one extensor, $P_e$ is expressed by

$$P_e = Ar_3 Ac_3 = Ar_2 Ac_2 = Ar_1 Ac_1 \tag{13}$$

Here, $Ac_1$ represents the antagonistic muscle activity of the DIP joint, and $Ac_2$ represents that of the PIP joint.

From Eq. (13), these values are calculated by

$$Ac_2 = \frac{Ar_3}{Ar_2} Ac_3 \tag{14}$$

$$Ac_1 = \frac{Ar_3}{Ar_1} Ac_3 \tag{15}$$

From Eqs. (14) and (15), $P_1$ and $P_2$ are given by

$$P_2 = (1 - Ar_2) Ac_2 = (1 - Ar_2) \frac{Ar_3}{Ar_2} Ac_3 \tag{16}$$

$$P_1 = (1 - Ar_1) Ac_1 = (1 - Ar_1) \frac{Ar_3}{Ar_1} Ac_3 \tag{17}$$

As mentioned above, we obtain $P_1$, $P_2$, $P_{3f}$, and $P_e$ when $\theta_1$, $\theta_2$, $\theta_3$, and $Ac_3 = P_{3f} + P_e$ are given.

### *3.6 Theoretical Proof of the Correspondence between Antagonistic Muscle Ratio and Joint Angle*

This section presents theoretical proof of the correspondence between antagonistic muscle ratio and joint angle described by Eq. (5). We begin by introducing the pneumatically driven musculoskeletal model depicted in Fig. 7.

We modeled the viscoelastic character of the pneumatic actuators as Kelvin-Voigt materials, and assumed that the properties of these actuators are the same (natural length: $x_0$). After being pressurized, the actuators are connected with a driving pulley at length $\bar{x}$. A robot link, inertia moment I, is attached to the pulley. When the pressure of the actuator is changed, the natural length of the actuator is changed to $\bar{\bar{x}}$. The actuators then generate contraction force in such a way that they try to contract at the length of $\bar{\bar{x}}$.

When the length of an extensor is $x_e$ and that of a flexor is $x_f$, the contraction force of the extensor $F_e$ and the flexor $F_f$ can be described by

$$F_e = k_e(x_e - \bar{\bar{x}}_e) - c_e\dot{x}_e, F_f = k_f(x_f - \bar{\bar{x}}_f) + c_f\dot{x}_f \tag{18}$$

where $k$ is an elastic coefficient, $c$ is a viscosity coefficient, and $x$ is the length of the actuator. Subscript $e$ is the parameter for the extensor, while $f$ is that for the flexor.

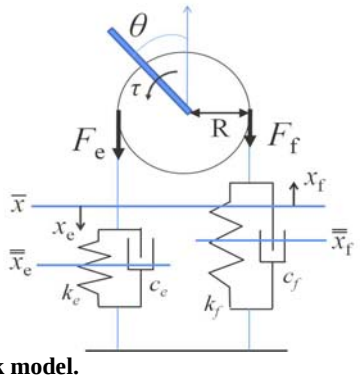


**Fig. 7 Link model.**

The link equation of the motion is

$$\mathrm{I}\ddot{\theta} = \mathrm{R}(F_e - F_f) \tag{19}$$

Substituting Eq. (18) into (19) and then rearranging it, we get

$$(\mathrm{I}/\mathrm{R})\ddot{\theta} = k_e(x_e - \overline{\overline{x}}_e) - c_e\dot{x}_e - k_f(x_f - \overline{\overline{x}}_f) - c_f\dot{x}_f \tag{20}$$

Assuming that actuators do not slip on the pulley,

$$\bar{x} - x_e = \mathrm{R}\theta\,, \quad x_f - \bar{x} = \mathrm{R}\theta \tag{21}$$

From Eq. (21),

$$x_e = -\mathrm{R}\theta + \bar{x}\,, \quad x_f = \mathrm{R}\theta + \bar{x} \tag{22}$$

$$\dot{x}_e = -\mathrm{R}\dot{\theta}, \quad \dot{x}_f = \mathrm{R}\dot{\theta} \tag{23}$$

Substituting Eqs. (22) and (23) into Eq. (20) and then rearranging it, we get

$$(\mathrm{I}/\mathrm{R})\ddot{\theta} = (c_e - c_f)\mathrm{R}\dot{\theta} - (k_e + k_f)\mathrm{R}\theta + (k_e - k_f)\bar{x} - k_e\overline{\overline{x}}_e + k_f\overline{\overline{x}}_f \tag{24}$$

Following [2], the contraction force is expressed by

$$F = (\pi \mathrm{r}_0^{\,2})P\mathrm{a}(1 - \beta\varepsilon)^2 - \mathrm{b} \tag{25}$$

where $P$ is the control pressure; $\varepsilon$ is the contraction ratio; and $\mathrm{r}_0$, a, b, and β are the intrinsic parameters of the actuators.

By applying the Taylor series of polynomials of degree 1 at $\varepsilon = 0$, Eq. (25) can be approximated by

$$F = P(\alpha - \beta\varepsilon) \tag{26}$$

where α and β are the intrinsic parameters of the actuators.

Since the contraction force of both flexor and extensor is zero during maximal contraction,

$$P_f(\alpha - \beta\varepsilon_f) = P_e(\alpha - \beta\varepsilon_e) \tag{27}$$

where

$$\varepsilon_e = \frac{x_0 - \overline{\overline{x}}_e}{x_0}\,, \quad \varepsilon_f = \frac{x_0 - \overline{\overline{x}}_f}{x_0} \tag{28}$$

Based on Eq. (26), the elastic coefficient of actuators is

$$k_e = \frac{\partial F_e}{\partial x_e} = \frac{\beta}{x_0}P_e\,, \quad k_f = \frac{\partial F_f}{\partial x_f} = \frac{\beta}{x_0}P_f \tag{29}$$

Substituting Eqs. (28) and (29) into Eq. (27) and then rearranging it, we get

$$-k_e\overline{\overline{x}}_e + k_f\overline{\overline{x}}_f = (\alpha - \beta)(P_e - P_f) = (\alpha - \beta)\frac{x_0}{\beta}(k_e - k_f) \tag{30}$$

Substituting Eq. (30) into Eq. (24), we get

$$(\mathrm{I}/\mathrm{R})\ddot{\theta} = (c_e - c_f)\mathrm{R}\dot{\theta} - (k_e + k_f)\mathrm{R}\theta + (k_e - k_f)\Omega \tag{31}$$

where $\Omega = \bar{x} + (\alpha\text{-}\beta)\,x_0/\beta$ is constant.

Provided that $\ddot{\theta} = \dot{\theta} = 0$, then rearranging above by $\theta$, we get

$$\theta = \frac{\Omega}{\mathrm{R}}\frac{k_e - k_f}{k_e + k_f} \tag{32}$$

From Eq. (29), the pressure ratio between $P_e$ and $P_f$ is equal to $k_e/k_f = P_e/P_f = r$. Therefore, the following denotes the relationship between $r$ and $\theta$.

$$\theta = \frac{\Omega}{\mathrm{R}}\frac{r-1}{r+1} \tag{33}$$

The relationship between antagonistic muscle ratio and joint angle is expressed as follows:

$$Ar = \frac{\theta - \theta_{\min}}{\theta_{\max} - \theta_{\min}} \tag{34}$$

Based on the definition of antagonistic muscle ratio, we get

$$\frac{P_e}{P_e + P_f} = \frac{1}{\theta_{\max} - \theta_{\min}}\theta - \frac{\theta_{\min}}{\theta_{\max} - \theta_{\min}} \tag{35}$$

Suppose that $\mathrm{A} = 1/(\theta_{max} - \theta_{min})$, $\mathrm{B} = -\theta_{min}/(\theta_{max} - \theta_{min})$:

$$\frac{P_e}{P_e + P_f} = \mathrm{A}\theta + \mathrm{B} \tag{36}$$

Rearranging the above,

$$\theta = \frac{(\frac{1-\mathrm{B}}{\mathrm{A}})P_e - \frac{\mathrm{B}}{\mathrm{A}}P_f}{P_e + P_f} \tag{37}$$

Suppose that $r = P_e/P_f$:

$$\theta = \frac{(\frac{1-\mathrm{B}}{\mathrm{A}})r - \frac{\mathrm{B}}{\mathrm{A}}}{r+1} \tag{38}$$

Assuming that

$$(1-\mathrm{B})/\mathrm{A} = \mathrm{B}/\mathrm{A} = \mathrm{D} \tag{39}$$

From Eqs. (38) and (39) we get

$$\theta = \mathrm{D}\frac{r-1}{r+1} \tag{40}$$

If Eq. (39) holds, A = 1/(2D) and B = 1/2. The model presented in section 3.3 is $\theta_{max}$ = 90deg and $\theta_{min}$ = -90deg. When we apply these angles to the definitions of A and B, A = 1/180 and B = 1/2. Therefore, Eqs. (39) and (40) hold under the model.

From the above, we proved the following propositions:

(1) The antagonistic muscle ratio *Ar* and the joint angle of the musculoskeletal joint model $\theta$ have the linear relationship expressed by Eq. (5);

(2) Regardless of antagonistic muscle activity *Ac*, the joint angle of the musculoskeletal joint model is determined by *Ar*.

## 4. Verification Experiment

### *4.1 Experiment Objective*

The objective here is to verify experimentally the basic idea of the proposed method by implementing the idea in the one-degree-of-freedom joint model introduced in section 2.2. This model was designed to be symmetrical and equipped with a one-degree-of-freedom joint and two McKibben pneumatic actuators.

### *4.2 Experiment Procedure*

- To avoid gravitational influence, the joint model was fixed on a flat table so that the flexion-extension plane was parallel to the surface of the table.
- The joint angle was set to 0deg when the joint was straightened, -90deg when the joint angle was minimum, and 90deg when the joint angle was maximum.
- We recorded the joint angle in step response, and measured the joint angle after 10sec as the steady-state value. For the measurement, we used the electromagnetic sensors called 3D Guidance developed by Ascension Technology Corp.
- We changed the desired angles from -90deg to 90deg in 10deg increments employing air pressures given by Eqs. (3)-(5). In this range of desired angles, we changed *Ac* following three patterns: 0.1 MPa, 0.15 MPa, and 0.2 MPa. The experiment was replicated over six trials in each pair of *Ar* (deducted from the desired joint angle) and *Ac*.

### *4.3 Results*

Fig. 8 provides the plots of $(\theta-\theta_{\min})/(\theta_{\max}-\theta_{\min})$. Here, $\theta$ is the steady-state value of the joint angle when *Ar* calculated from the desired angle is given. A continuous line in Fig. 8 represents a linear approximation of the plot; a dashed line represents the theoretical formula expressed by Eq. (5).

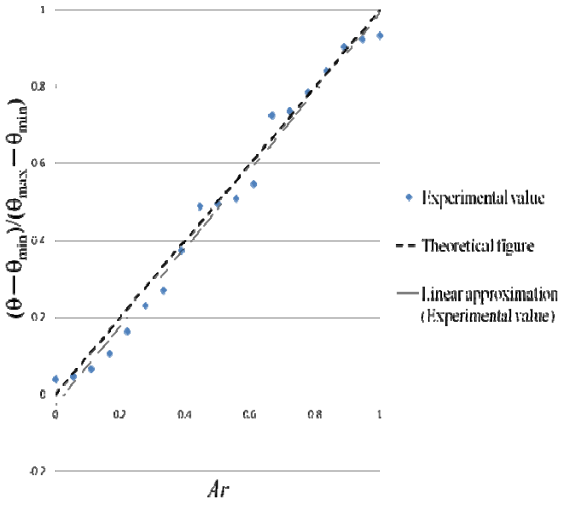


**Fig. 8 Correspondence between ($\theta$ - $\theta_{min}$)/ ($\theta_{max}$ - $\theta_{min}$) and *Ar* (*Ac* = 0.15 MPa, 1st trial).**

Fig. 9 provides the plots of steady-state values of the joint angle against *Ar* calculated from the desired angle. We used three values for *Ac*: 0.1 MPa, 0.15 MPa, and 0.2 MPa.

### *4.4 Discussion*

To validate the proposed method, we analyzed the relationship between *Ar* and joint angle, and the independence of *Ar* and *Ac*.

First, we analyze the relationship between *Ar* and joint angle. The determination coefficient between the experiment value and its linear approximation in Fig. 8 was approximately 0.98 on average from the six trials. This means that the experiment results fit the linear approximation well. Therefore, *Ar* and joint angle are linearly related. The linear approximation and the theoretical formula varied slightly. This observed discrepancy can be explained by the fact that the properties of the flexor and the extensor were different in reality. Despite the effort to produce identical products, the qualities of the actuator properties cannot be identical when they are manufactured.

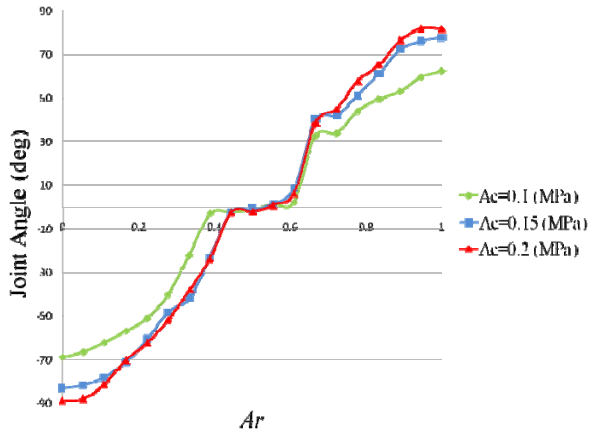


**Fig. 9 Comparison of steady-state joint angles among different antagonistic muscle activities (1st trial).**

Second, we focus on the independence of *Ar* and *Ac*. In Fig. 9, the plot in *Ac* = 0.15 MPa was in accord with the plot in *Ac* = 0.2 MPa. Therefore, we concluded that *Ar*, corresponding to joint angle, was independent of *Ac*, corresponding to joint stiffness. The plot in *Ac* = 0.1 MPa was inconsistent with the other two plots. This discrepancy indicates that *Ac* = 0.1 MPa is below the value of $\overline{P}$ in Eq. (2). We observed similar patterns in the other trials.

## 5. Joint Angle Control Experiment (1DOF Model)

### *5.1 Experiment Objective*

The objective here is to implement the proposed method in the one-degree-of-freedom joint model and examine the joint angle control. The evaluation criterion is accuracy in following the desired angle.

### *5.2 Experiment Procedure*

- To avoid gravitational influence, the one-degree-of-freedom joint model was fixed on a flat table so that the flexion-extension plane of the model was parallel to the surface of the table.
- The joint angle was set to be 0deg when the joint was straightened, -90deg when the joint angle was minimum, and 90deg when the joint angle was maximum.
- We recorded the step response of the joint angle. The joint angle was measured by the electromagnetic sensors, 3D Guidance developed by Ascension Technology Corp. We changed *Ac* following two patterns: 0.15 MPa and 0.2 MPa.
- The PID gains were experimentally tuned to give the best tracking response at *Ac* = 0.15 MPa, desired angle of -60deg.
- The experiment was replicated over five trials.

### *5.3 Results*

Figs. 10-11 plot the time series of the step response of the joint angle. Table 5 indicates the PID gains in the step response.

In each figure, the dotted lines denote the response of *Ac* = 0.15 MPa, and the long-dashed lines denote the response of *Ac* = 0.2 MPa. For comparison, we also illustrate the result of the feedforward control in Figs. 10-11 (continuous lines). The results presented in these two figures are the third trial. We observed similar patterns in the other trials.

### *5.4 Discussion*

In this section, we discuss positioning accuracy and steady-state joint angle of feedback control.

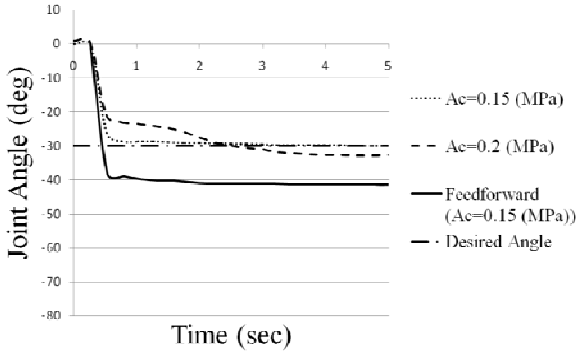


**Fig. 10 Step response: -30deg (3rd trial).**

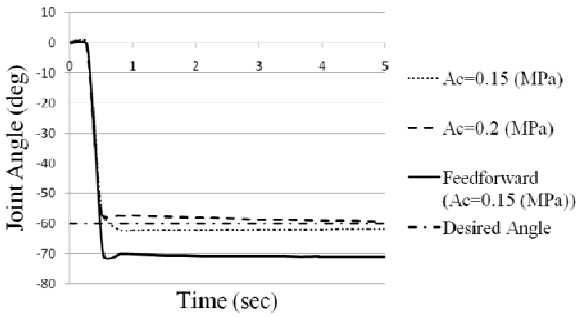


**Fig. 11 Step response: -60deg (3rd trial).**

**Table 5 Parameters of PID controller (step response).**

| $K_P$ | $K_I$ | $K_D$ |
|---|---|---|
| 0.51 | 1.85 | 0.03 |

First, we analyzed positioning accuracy. It is obvious that steady-state errors remained in the feedforward control (Figs. 10-11), due to the joint structure difference between the theoretical model and the actual model. In section 3, we assumed that the actuators are connected with a driving pulley; thus, the moment arms should be constant. However, the actual robot structure does not fully replicate the theoretical one in terms of the moment arms. The joint needs to be more extended (Figs. 10-11), because the moment arm of the flexor is longer than that of the extensor (Fig. 12), resulting in dominance of the flexor in terms of moment. These errors were clearly reduced by implementing the feedback control.

Secondly, we analyzed the steady-state joint angle. Due to joint friction, the steady-state errors remained even when we applied the feedback control (Figs. 10-11). When the joint is lubricated with oil, the joint may converge to the desired joint angle.

## 6. Joint Angle Control Experiment (Five-Fingered Robot Hand)

### *6.1 Experiment Objective*

The objective here is to implement the proposed method in the index finger of the five-fingered robot hand and examine the performance of the joint angle control. The evaluation criteria are accuracy in following the desired angle and quick response.

### *6.2 Experiment Procedure*

- To avoid gravitational influence, the five-fingered robot hand was fixed on a flat table so that the flexion-extension plane of the index finger was parallel to the surface of the table.
- Joint angles of the robot were set to be 0deg when the joint was extended and the finger was parallel to its parent link. When the joint flexed, the joint angle was negative. The initial condition was the full extension of all the joints.

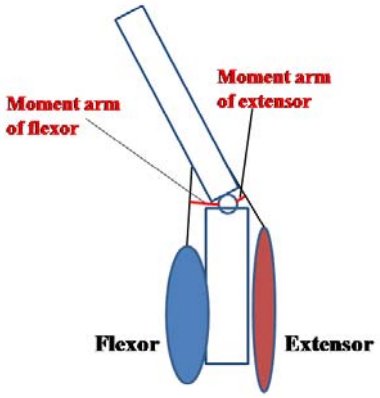


**Fig. 12 Different moment arms between extensor and flexor.**

- We recorded the step response of the joint angle of the index finger. The joint angles were measured using the data glove called ShapeHand developed by Measurand, Inc.
- $Ac_3$ was fixed to 0.2 MPa. The desired angles were -25deg for the DIP joint, -30deg for the PIP joint, and -40deg for the MP joint.
- We delayed the output pressure of the actuators driving the MP joint for 0.5 sec after trials without any delay of the actuators. These actuators are represented as $P_{3f}$, $P_e$ in Fig. 6.

### *6.3 Results*

Figs. 13-15 plot the time series of step response of the joint angle (DIP joint, PIP joint, and MP joint). The dotted lines denote the response without any actuator delay, and the continuous lines denote the response when the actuators driving the MP joint were delayed for 0.5 sec.

### *6.4 Discussion*

In this section, we analyze delaying activation of actuators, positioning accuracy, and quickness of response.

First, we focus on delayed activation of the actuators. The continuous lines in Figs. 13-15 have greater accuracy in following the desired angle than the dotted line. These results indicate that the extensor ($P_e$ in Fig. 6) interrupted the flexion movement of the DIP and PIP joints when the actuators were activated

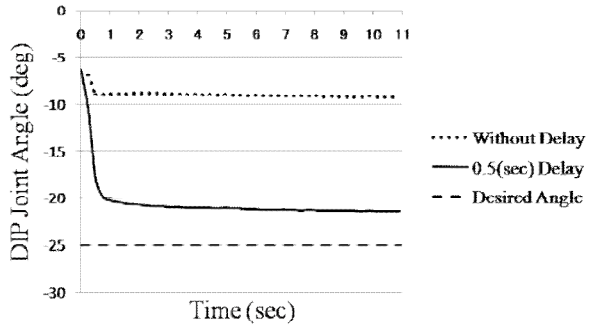


**Fig. 13 Step responses of the DIP joint: -25deg.**

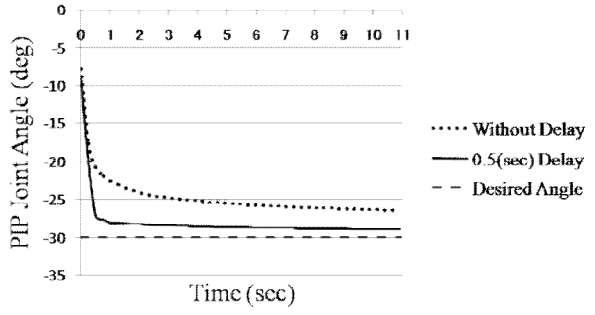


**Fig. 14 Step responses of the PIP joint: -30deg.**

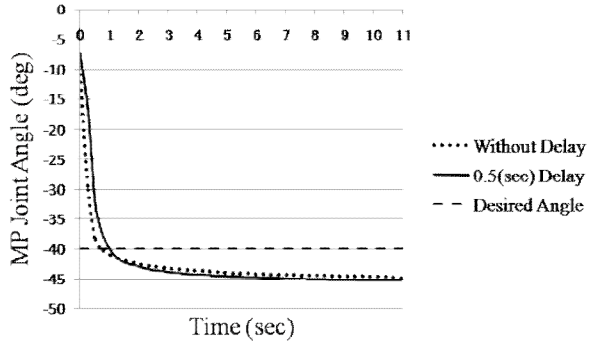


**Fig. 15 Step responses of the MP joint: -40deg.**

simultaneously because the extensor was longer than the flexors of the DIP and PIP joints, resulting in the dominance of the extensor in terms of its axial force.

Second, we investigate positioning accuracy. It is obvious that steady-state errors remained in all results (Figs. 13-15). We assume that the discrepancy results from the difference between theoretical and actual models. In section 3, we assumed that the joint structure of the joint model was bilaterally symmetric and that the actuator properties were identical. However, the actual robot hand does not replicate the theoretical one in terms of symmetry. In reality, the DIP and PIP joints were less flexed (Figs. 13-14). We assume that this is due to the dominance of the extensor, as mentioned above.

However, according to the theory, the MP joint was supposed to be more extended (Fig. 15) because the moment arm of the flexor was longer than that of the extensor (Fig. 12), resulting in the dominance of the flexor moment.

Third, we investigate the quickness of the response. A human moves the index finger up to 5.5 Hz. The response of the robot hand was inferior to that of the human. In order to achieve quick response, we need to expand the inner diameter of the air tube and shorten it as well.

## 7. Conclusions

This paper has proposed and demonstrated a joint angle control method of a pneumatically driven musculoskeletal model. The basic concept of the biologically inspired method is that the joint angle corresponds to the coordination of the antagonistic muscle pair. We defined coordination based on the parameters antagonistic muscle ratio and antagonistic muscle activity. Antagonistic muscle ratio is expressed by the ratio of air pressures between the extensor and the sum of the extensor and the flexor. Antagonistic muscle activity is expressed by the sum of air pressures of the extensor and the flexor. In the theoretical analysis, we verified that (1) antagonistic muscle ratio and joint angle are linearly related, and (2) antagonistic muscle ratio and antagonistic muscle activity are independent. This trend was empirically demonstrated using a one-degree-of-freedom joint model. Our model was able to behave as in theory, provided that no external force was applied. We also developed the PID feedback control, implemented it in the one-degree-of-freedom joint model, and examined its step response. Results indicated improved accuracy compared to that of the feedforward control.

Furthermore, we implemented feedforward control in the index finger of the five-fingered robot hand and examined the step response. Results indicated remaining steady-state errors due to the difference

between the theoretical model and the actual one.

In our future research, we will target (1) parameter correction in the correspondence between antagonistic muscle ratio and joint angle for the five-fingered robot hand, and (2) implementation of the proposed feedback control in the five-fingered robot hand.

## Acknowledgments

This research was conducted in collaboration with SQUSE Co., Ltd. (Kyoto, Japan) and supported by Grants-in-Aid for Scientific Research (Project Number 23360112 and 23560524) of the Japan Society for the Promotion of Science.

## References

[1] R. Richardson, M. Brown, B. Bhakta, M. Levesley, Impedance control for a pneumatic robot-based around pole-placement, joint space controllers, Control Engineering Practice 13 (3) (2005) 291-303.

[2] B. Tondu, P. Lopez, Modeling and control of McKibben artificial muscle robot actuators, IEEE Control Systems Magazine 20 (2) (2000) 15-38.

[3] N.A. Bernstein, The Coordination and Regulation of Movement, Pergamon Press, 1967.

[4] P.L. Gribble, L.I. Mullin, N. Cothros, A. Matter, Role of cocontraction in arm movement accuracy, Journal of Neurophysiology 89 (2003) 2396-2405.

[5] N. Tsujiuchi, T. Koizumi, S. Nishino, H. Komatsubara, T. Kudawara, M. Hirano, Development of pneumatic robot hand and construction of master-slave system, Journal of System Design and Dynamics 2 (6) (2008) 1306-1315.

[6] J. Schröder, K. Kawamura, T. Gockel, R. Dillmann, Improved control of humanoid arm driven by pneumatic actuators, in: Proceedings of IEEE-RAS Int. Conf. on Humanoid Robots (Humanoids), 2003.

[7] R.Q. van der Linde, Design, Analysis, and control of a low power joint for walking robots by phasic activation of McKibben muscles, IEEE Transactions on Robotics and Automation 15 (4) (1999) 599-604.

[8] N. Tsujiuchi, T. Koizumi, S. Shirai, T. Kudawara, Y. Ichikawa, Development of a low pressure driven pneumatic actuator and its application to a robot hand, in: Proceedings of the 32nd Annual Conf. of the IEEE Industrial Electronics Society (IECON), 2006, pp. 3040-3045.

[9] Y. Honda, F. Miyazaki, A. Nishikawa, Control of pneumatic five-fingered robot hand using antagonistic muscle ratio and antagonistic muscle activity, in: Proceedings of the 3rd IEEE RAS-EMBS Int. Conf. on Biomedical Robotics and Biomechatronics (BioRob), 2010, pp. 337-342.

[10] Y. Honda, F. Miyazaki, A. Nishikawa, Angle control of pneumatically-driven musculoskeletal model using antagonistic muscle ratio and antagonistic muscle activity, in: Proceedings of the IEEE Int. Conf. on Robotics and Biomimetics (ROBIO), 2010, pp. 1722-1727.